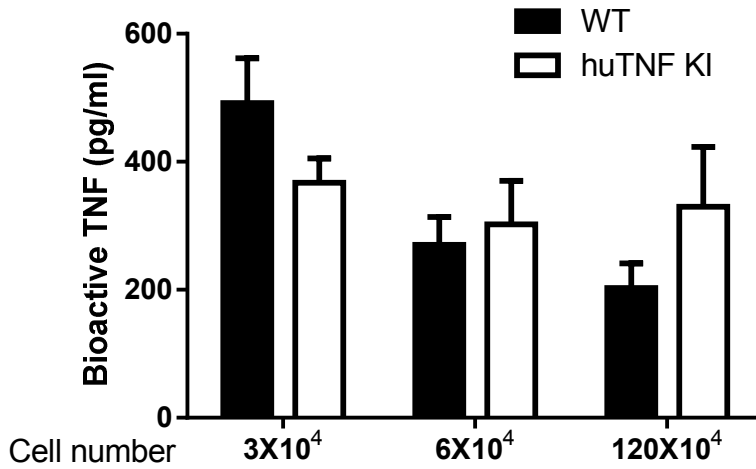


**Supplemental Figure 1.** Structure of *tnf* locus in huTNF knock-in mice. Top and middle lanes: schematic representation mouse and human loci, respectively, showing exons of TNF and lymphotoxin genes and location of the breakpoints.

Bottom lane: huTNF knock-in locus with BsPH1 restriction site and single *loxP* recombination site (remaining after Cre-mediated removal of the neomycin resistance cassette) at the mouse/human and human/mouse junctions. Mouse and human portions of the loci are marked with green and magenta colors, respectively.

A



B

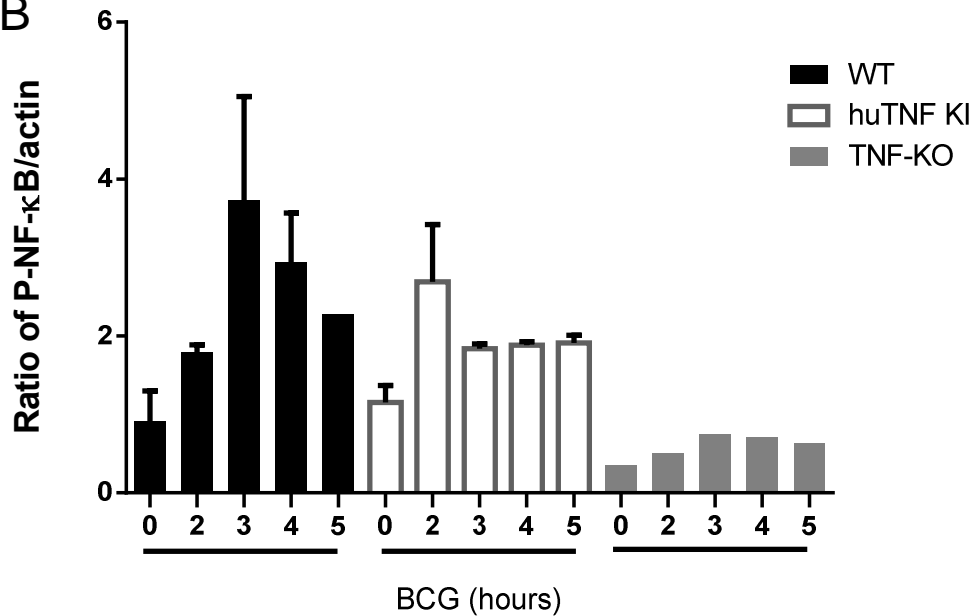


Fig. S2. BMDMs from humanized TNF KI mice respond as well as WT cells producing similar amounts of bioactive TNF after BCG infection.

(A) Bioactive TNF tested in WEHI164 cells in culture supernatants from BMDMs plated at different concentrations (96 well plates) as indicated, infected with BCG at MOI 1 for 24 h.

Data are represented as mean  $\pm$  SEM ( $n = 6$ ). No statistically significant differences were observed between WT and huTNF KI cell supernatants.

(B) Ratio of phosphorylated p65 NF-κB/actin on Western blot using Quantity One<sup>®</sup> analysis software on two different experiments ( $n = 2$  for WT and huTNF KI and 1 for TNF KO mice).

Bar graphs show mean  $\pm$  SEM.

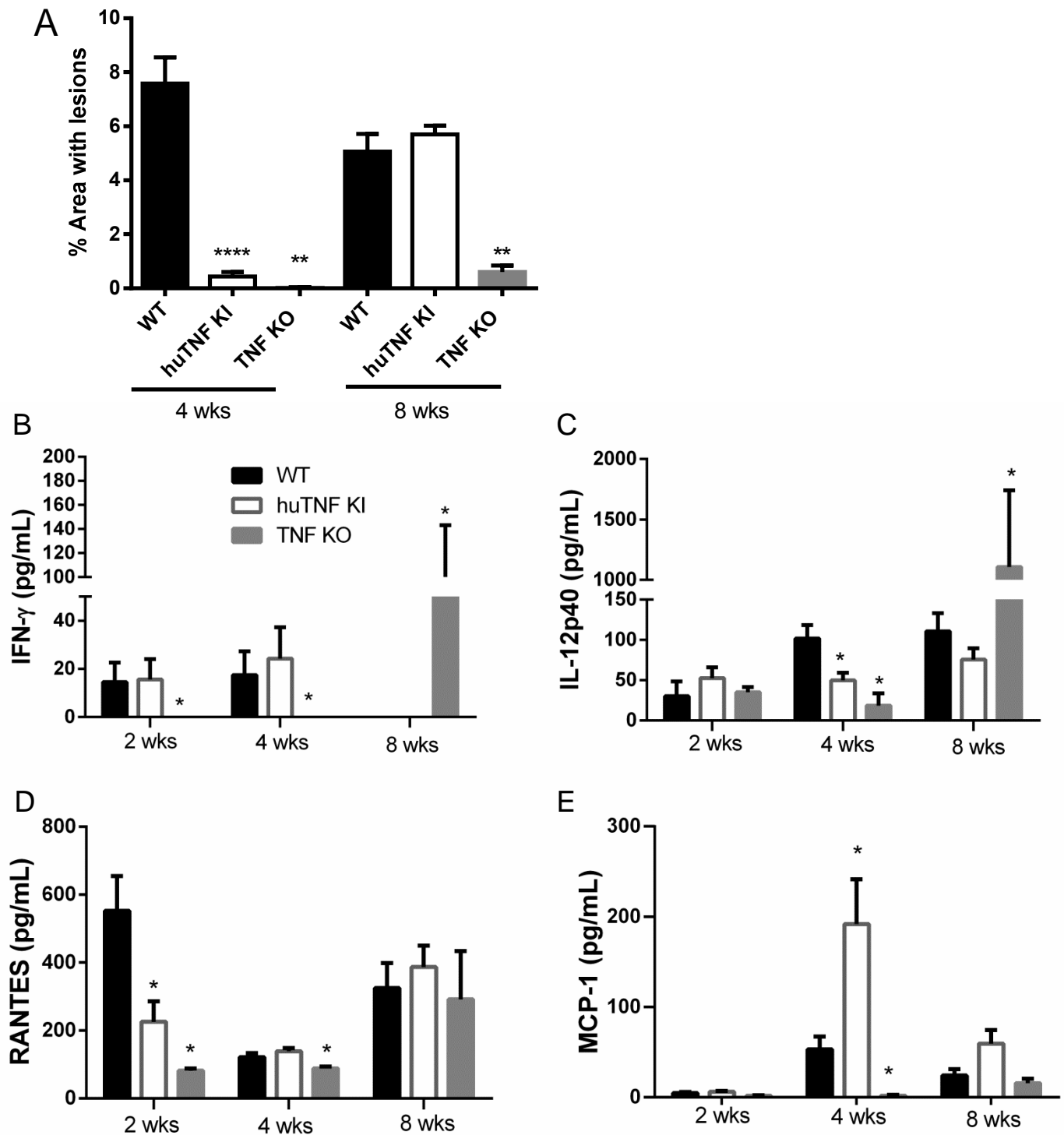
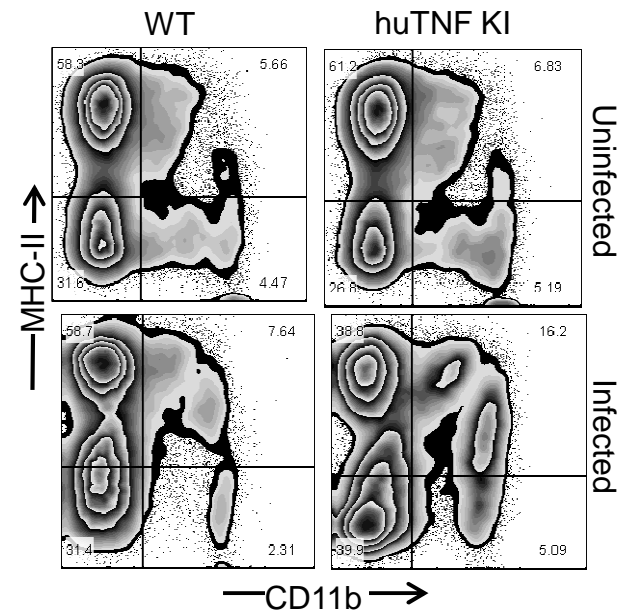
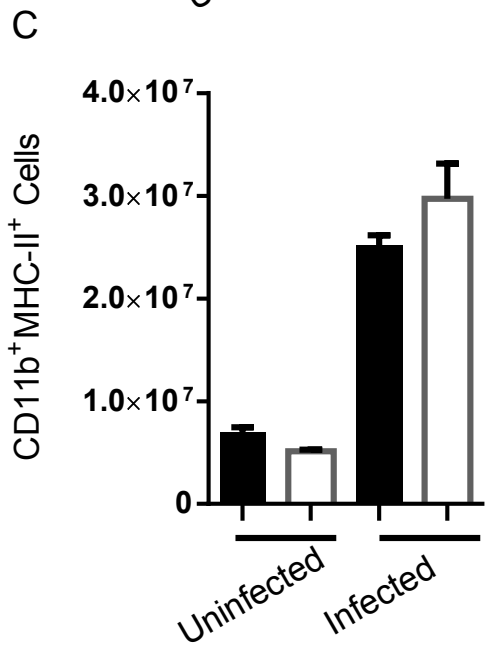
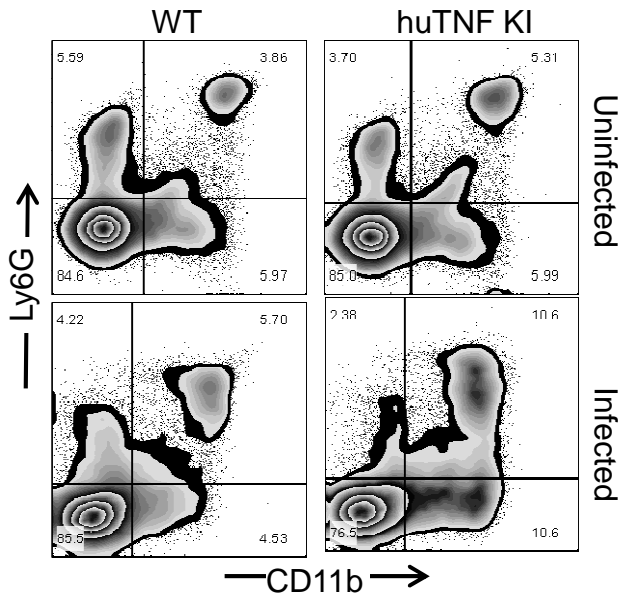
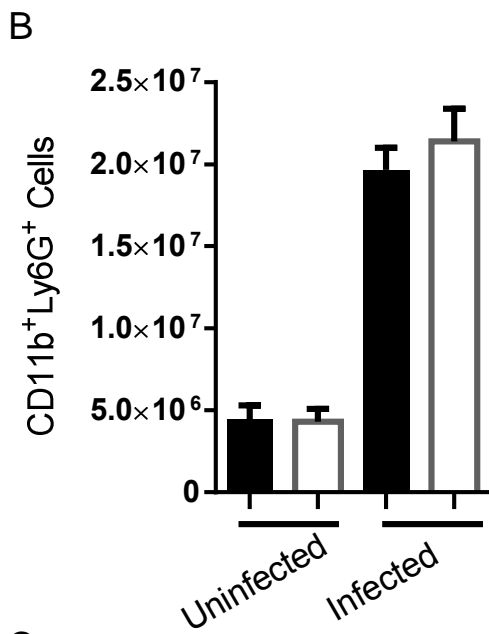
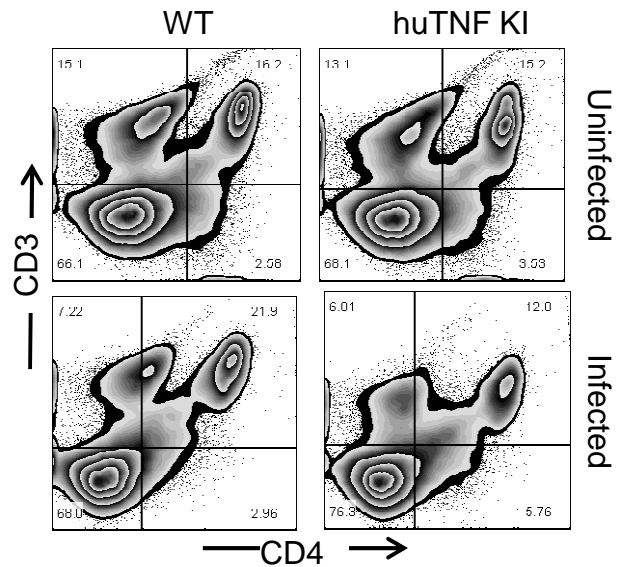
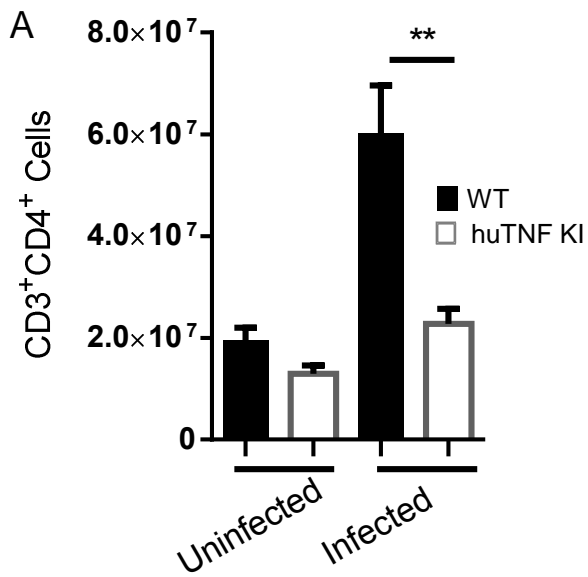


Fig. S3. Liver pathology and cytokine levels in the serum of huTNF KI, TNF KO and WT mice after 4 and 8 weeks of BCG infection. (A) Liver areas with lesions represented as percentage corresponding to area of granulomas / area surface of total liver which was  $50 \pm 11 \text{ mm}^2$  per liver section and animal ( $n = 7-5$  for WT and huTNF KI, and 3 for TNF KO mice). Bar graphs show mean  $\pm$  SD. \*\*\*\*  $p < 0.0001$ , \*\*  $p < 0.005$  versus WT.

(B) IFN- $\gamma$ , (C) IL-12p40, (D) RANTES, and (E) MCP-1 serum levels assessed at 2, 4, and 8 weeks postinfection ( $n = 4-9$  mice/group). Bar graphs show mean  $\pm$  SEM. \*,  $p < 0.05$  versus WT.



Supplemental Figure S4

Fig. S4. Changes in splenic CD4 T cells, neutrophils and macrophages after BCG infection. FACS analyses of splenocytes obtained from uninfected and 4 weeks BCG-infected mice. (A) Absolut number of CD3<sup>+</sup>CD4<sup>+</sup> cells gated on viable cells was obtained according to total number of splenocytes/spleen, (B) Absolut number of CD11b<sup>+</sup>Ly6G<sup>+</sup> (neutrophils) and (C) CD11b<sup>+</sup>MHC-II<sup>+</sup> (macrophages) cells obtained according to total number of splenocytes/spleen (*n* = 4 mice/ group). Representative zebra plot of CD3<sup>+</sup>CD4<sup>+</sup> cells, CD11b<sup>+</sup>Ly6G<sup>+</sup> cells or CD11b<sup>+</sup>MHC-II<sup>+</sup> cells from spleen of uninfected and 4 weeks BCG-infected mice. Bar graphs show mean  $\pm$  SEM. \*, *p*<0.05, \*\*, *p*<0.01 versus WT.

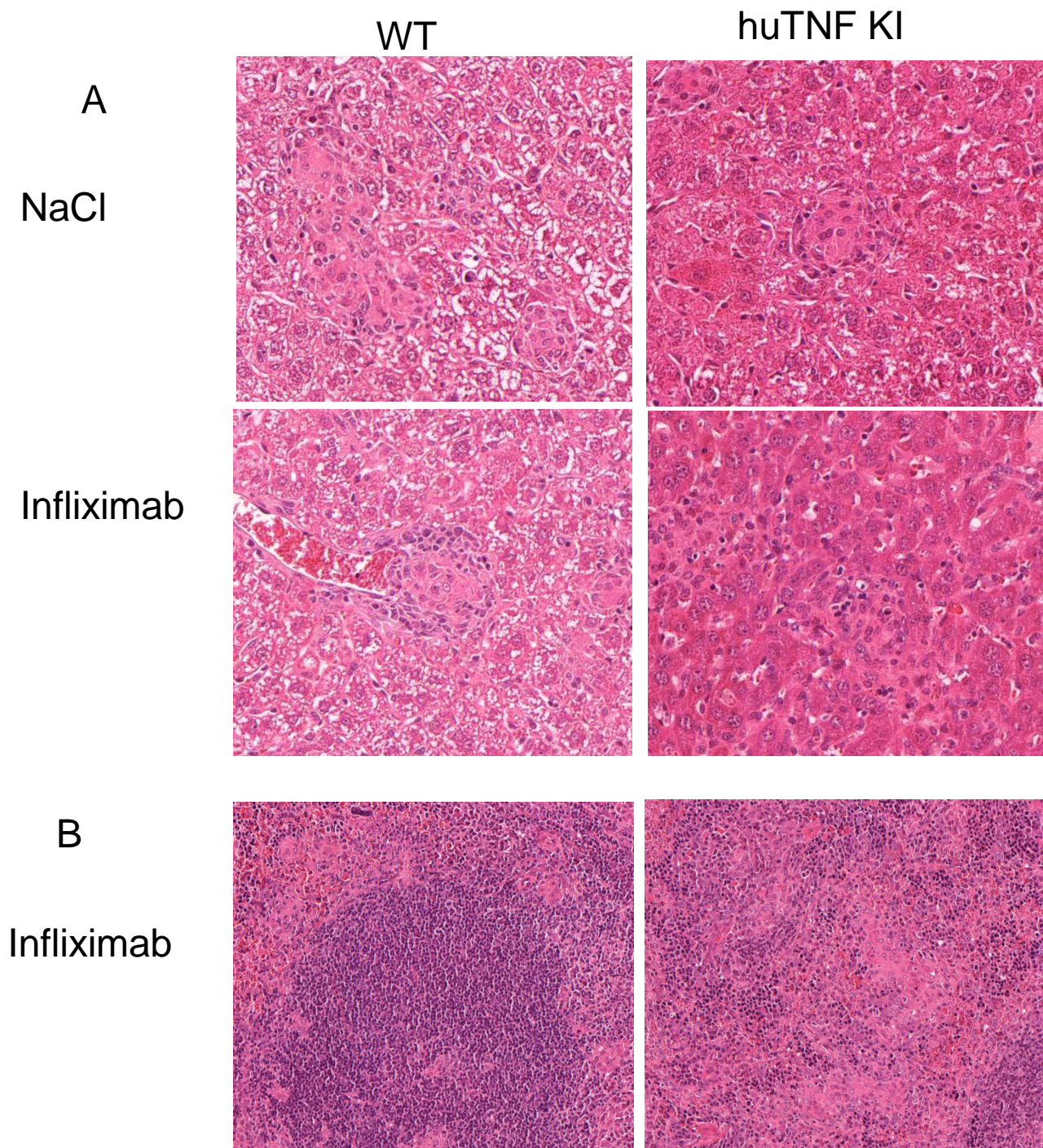


Fig. S5. Liver and spleen sections (H&E) from 4 weeks BCG-infected mice and treated with vehicle or Infliximab.

(A) Liver section from WT and huTNF KI mice treated with either diluent or Infliximab.

(B) Spleen section of WT and huTNF BCG-infected and treated with Infliximab